Multi-Impulse Input Shaper for Vibration Control with Smoothness-Adjustability

Abdullah A. Alshaya

***Abstract*— A new control technique based on input-shaping principle is proposed for limiting the residual vibrations of flexible dynamic systems. Commanding flexible systems with unshaped reference inputs can lead to unwanted vibrations that may compromise the system's integrity. To address this, input shapers are employed by modifying the system's input command to reduce residual vibrations while ensuring the system reaches its target position within a short maneuver time. However, convolving a classical input shaper, such as zero-vibration (ZV) or zero-vibration-derivative (ZVD) input shaper, with a reference step or pulse command can produce shaped commands with abrupt jumps, which may negatively impact the system's actuator. When versine, S-curve, or polynomial profiles are used as reference inputs in order to have smooth shaped profile after convolution with the classical input shapers, the generated commands tend to have prolonged maneuver times. To overcome these limitations in the classical input shapers, the proposed control technique introduces a multi-impulse input shaper that, upon convolution, generates a smooth shaped command without compromising maneuver time, while fully utilizing the system's maximum input capability.**

I. INTRODUCTION

Controlling systems by means of passive and active control methods involving flexibility attracts many researchers across various fields [1]. Feedback and open-loop control are the most common approaches within active controlling methods, with the former requiring sensors to capture the state of the system under consideration. For well-defined systems, open-loop control methods are typically implemented in applications that demand precise positioning, fast maneuvering, and safe operation. Several controlling methods were used to control flexible systems such as tower crane system [2], [3], overhead crane system [4], flexible manipulator system [5], [6], or even systems having fluid sloshing [7]. The input-shaping controller, which functions as a prefilter for the system, is widely used due to its simplicity [8], [9], [10], ease of design and implementation [11], [12], minimal time penalty [13], robustness to system uncertainties [14], [15], and its applicability to both linear and nonlinear systems [11], [16], [17], [18], as well as single-mode and multi-mode system [19], [20], [21], [22]. Furthermore, the input shaping controller was applied to a system with time-varying parameter; a traveling overhead crane with hoisting/lowering maneuver [23]. Even though the residual vibration was not completely suppressed, the implementation of such controller helps in reducing the residual vibration. The input shaper controller can be easily implemented in closed loop system with other controlling approaches [24], [25], [26].

*This work was not supported by any organization.

Mechanical Engineering Department, College of Engineering and Petroleum, Kuwait University, PO Box 5969, Safat 13060, Kuwait abdullah.alshaye@ku.edu.kw

Input-shaping technique is based on convolving what is known as input shapers, $s(t)$, with the system's reference input, $r(t)$, to form a shaped command, $f(t) = r(t) * s(t)$, that commands the system without inducing residual vibration, Figure 1. If the reference input has a step or pulse profile, the produced shaped command after convolution with the input shapers consists of abrupt jumps, which may negatively impact the system's actuator because of the substantial requirement of inrush currents. Using versine, S-curve, or polynomial profiles as reference inputs, the generated shaped command tends to have prolonged maneuver time [27], [28], [29].

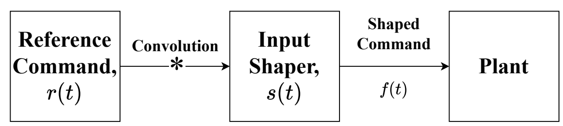

Fig. 1: Flowchart of input shaping techniques.

Unlike the classical input-shaping techniques, one can directly engineered shaped commands that satisfy the system and input requirements by means of optimal control approach [4]. This process is usually referred to as command-shaping technique. Several discrete and continuous profiles have been used to design a shaped command for vibration reduction of payload oscillation in overhead crane and sloshing suppression of induced water sloshing. General profiles in the form of multi-steps [7], [30], polynomial [31], [32], and wave forms [32], [33], [34], [35] were utilized. These shaped commands from such profiles are required to be designed prior implementation, and strong actuators are needed to ensure that the commanded system follows the predefined designed trajectory.

Even though the optimal control, e.g. command shaping process, recently proves its capability in controlling flexible systems [36], [37], the ease of implementation of input shaping that is based on convolution process makes it still an appealing controlling approach. To overcome the limitations of fixed shaper duration and prolonged shaped command when convolving a classical input shaper with smooth reference commands, the present work demonstrates a novel approach in generating a smooth shaped command from a multi-impulse input shaper and regardless of the reference input profile, while ensuring utilizing the system's maximum input capability to have an optimum maneuver. The proposed technique combine the advantageous of the input shaper that can be convolved with any reference input command and the advantageous of the command shaping that can be designed to have fast response as well as ensure utilizing system's driven capability.

II. Input Shaping Technique

Since a single impulse serves as the fundamental component for constructing any arbitrary function, a sequence of carefully designed impulses, known as the *input shaper*, $s(t)$, can be utilized to create inputs that minimize vibration. This is accomplished by convolving the desired input, $r(t)$, with the input shaper, yielding a shaped input, $f(t) = r(t) * s(t)$, which enables the system to follow the reference command without generating residual vibrations (see Figure 1). Consequently, the initial step in designing input shapers that ensure a vibration-free system response involves analyzing the system's behavior when subjected to multiple impulse inputs.

A. Response of a Multi-Impulse Input

A multi-impulse input shaper, $s(t)$, of M impulses is considered,

$$s(t) = \begin{bmatrix} A_1 & A_2 & \cdots & A_M \\ t_1 & t_2 & \cdots & t_M \end{bmatrix} \tag{1}$$

where A_j for $j = 1,2,\ldots,M$ are the magnitude of the jth impulse, and t_j is time location of the impulse A_j. The decaying sinusoidal response of a second-order linear underdamped vibratory system with a natural frequency of ω_n and a damping ratio of ζ_n when it is subjected by the M-impulse input of Eq. (1) is [14]:

$$y(t) = \sum_{j=1}^{M} \left[\frac{A_j \exp\left[-\zeta_n \omega_n (t - t_j)\right]}{\omega_n \sqrt{1-\zeta_n^2}} \right] \sin\left[\omega_n \sqrt{1-\zeta_n^2}\,(t - t_j) \right] \tag{2}$$

Since the objective of the input shaper is to eliminate the induced residual vibration of the commanded vibratory system of Eq. (2), the magnitude of the residual vibration at the end of the last impulse must be diminished. Hence,

$$A_{\text{res}} = \frac{\exp\left(-\zeta_n \omega_n t_M\right)}{\omega_n \sqrt{1-\zeta_n^2}} \sqrt{\left[C(\omega_n, \zeta_n)\right]^2 + \left[S(\omega_n, \zeta_n)\right]^2} \tag{3}$$

where

$$C(\omega_n, \zeta_n) = \sum_{j=1}^{M} A_j \exp\left(\zeta_n \omega_n t_j\right) \cos\left(\omega_n \sqrt{1-\zeta_n^2} t_j \right) \tag{4a}$$

$$S(\omega_n, \zeta_n) = \sum_{j=1}^{M} A_j \exp\left(\zeta_n \omega_n t_j\right) \sin\left(\omega_n \sqrt{1-\zeta_n^2} t_j \right) \tag{4b}$$

To have $A_{\text{res}} = 0$, it requires that $C(\omega_n, \zeta_n) = 0$ and $S(\omega_n, \zeta_n) = 0$. Since the shaped command is produced by convolving the input shaper with the system's reference command, the total and cumulative sum of the input shaper's impulses should be equal to and less than one, respectively,

$$\sum_{j=1}^{M} A_j = 1, \qquad \text{and} \qquad \left| \sum_{j=1}^{k} A_j \right| \leq 1 \tag{5}$$

for $k = 1,2,\ldots,M$. Theses two conditions ensure that the shaped command reaches the set-point and do not exceed the input capability, respectively.

B. Zero-Vibration (ZV) Input Shaper

The minimum number of impulses needed to satisfy the zero residual vibration as well as Eq. (5) is $M = 2$. Upon solving the aforementioned constraints while ensuring minimum shaper duration, i.e., $\min(t_2)$, the following two-impulse shaper, known as the zero-vibration (ZV) input shaper, has a form of [14]:

$$\text{ZV} = \begin{bmatrix} A_i \\ t_i \end{bmatrix} = \begin{bmatrix} \frac{1}{K+1} & \frac{K}{K+1} \\ t_1 & t_1 + \Delta T \end{bmatrix} \tag{6}$$

where $K = \exp\left(-\pi\zeta_n / \sqrt{1-\zeta_n^2}\right)$, ΔT is the half period of the damped system, i.e., $\Delta T = \tau_d/2 = \pi/\omega_d$, and t_1 is the time location when the input shaper is activated.

III. Smooth Input Shaper

One can observe from the constraint equations of the zero residual vibration that the resultant equations are nonlinear in terms of A_j and t_j. Furthermore, the values of t_j may not match the sampling time of the system's driven motor, and the differences between the adjacent impulses, $A_{j+1} - A_j$, may be large which require substantial inrush current from the driven motor.

A. Input Shaper with Equidistant Time Interval

To resolve the issue of mismatching that could occur if the time locations of the impulses are not within the sampling time of the driven motor, the sequence of the M impulses input shaper is assumed to have equidistant time interval, $\Delta t = t_{j+1} - t_j = t_j - t_{j-1}\ \forall j$. The constraint equations of the zero residual vibration become:

$$\sum_{j=1}^{M} A_j \exp\left[(j-1)\zeta_n \omega_n \Delta t\right] \cos\left((j-1)\omega_n \sqrt{1-\zeta_n^2}\Delta t \right) = 0 \tag{7a}$$

$$\sum_{j=1}^{M} A_j \exp\left[(j-1)\zeta_n \omega_n \Delta t\right] \sin\left((j-1)\omega_n \sqrt{1-\zeta_n^2}\Delta t \right) = 0 \tag{7b}$$

It is clear that Eqs. (7) can be written as a linear set of simultaneous equations in terms of the input shaper's impulses, A_j, for a given value of Δt. The user should select the time interval between the impulses of the input shaper to ensure it matches the sampling time of the system's driven motor.

B. Three-impulse Input Shaper

The minimum number of impulses needed to satisfy the zero residual vibration of Eq. (7) and the normalization constraint equation of Eq. (5) is $M = 3$ for any arbitrary value of t_1 and Δt. Figure 2 shows four different input shapers designed for undamped system ($\zeta_n = 0$) with different time interval, Δt. The absolute values of the input shaper's impulses with a time interval of $\Delta t = \tau_n/6$, Figure 2a, are 1.

Therefore, this input shaper of Figure 2a is known as the unity-magnitude input shaper (UMZV). The input shaper corresponds to a time interval of $\Delta t = \tau_n/4$, Figure 2b, is the classical ZV input shaper, Eq. (6). For a time interval of $\Delta t = \tau_n/3$, the resultant input shaper of Figure 2c has equal impulses, $A_j = 1/3\ \forall j$. Finally, the input shaper with a time interval of $\Delta t = \tau_n/2$ in Figure 2d is the robust version of ZV input shaper, which is known as the zero vibration and derivative (ZVD) input shaper.

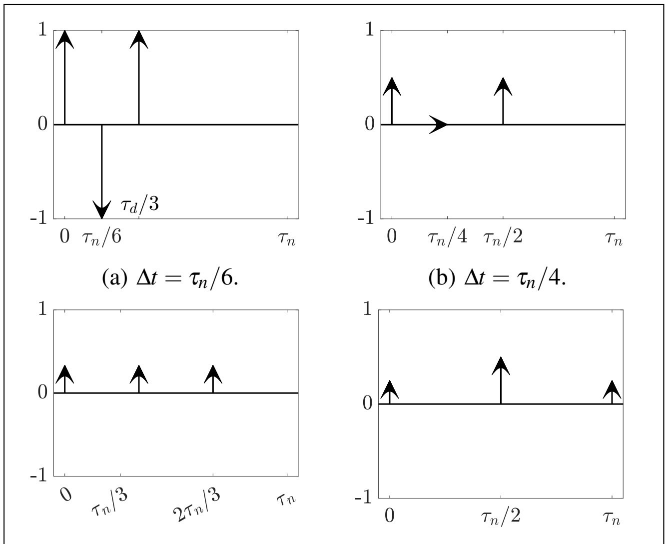

(a) $\Delta t = \tau_n/6$. (b) $\Delta t = \tau_n/4$. (c) $\Delta t = \tau_n/3$. (d) $\Delta t = \tau_n/2$.

Fig. 2: Three-impulse input shaper with different shaper time interval, Δt, for undamped system ($\zeta_n = 0$); the horizontal arrow corresponds to a zero impulse.

It is worth mentioning that the 3-impulse input shaper in Figure 2, for a given shaper duration of $3\Delta t$, was determined by simultaneously solving a set of three linear equations for the impulse magnitudes A_j, where $j = 1,2,3$, Eqs. (7). Therefore, the assumption of an equidistant multi-impulse input shaper not only resolves the mismatch issues but also eliminates the need for numerical optimization to solve the set of nonlinear equations in Eqs. (4). Furthermore, if the considered vibratory system is multi-mode, Eqs. (7) can be easily extended and be applied for each of the vibrational modes in order to design a multi-impulse multi-mode input shaper. Finally, the sensitivity of the equidistant multi-impulse input shaper can be enhanced by additionally imposing constraints for widening the robustness range such as enforcing the derivative of the residual vibration amplitude at the modeled system parameters to be zero.

C. Smoothing the Input Shaper

The objective is to develop a sequence of impulses for an input shaper that if convolved with any reference input, the generated command will have a smooth profile. The input shaper of Eq. (1) can be designed such that three of its impulses are needed to satisfy the constraint equations of Eqs. (5) and (7), where the remaining excess impulses are used to minimize the difference between any two adjacent impulses. With simple manipulation, one can write the constraint equations in a matrix form as:

$$\mathbf{J}_1\mathbf{a}_1 + \mathbf{J}_2\mathbf{a}_2 = \mathbf{b} \tag{8}$$

where $\mathbf{J}_1 \in \mathbb{R}^{3\times 3}$ is a square matrix whose indices are the left sides of Eqs. (5) and (7), $\mathbf{a}_1 \in \mathbb{R}^{3\times 1}$ is a vector containing three impulses that ensure the satisfaction of constraint equations of Eqs. (5) and (7), $\mathbf{J}_2 \in \mathbb{R}^{3\times N}$ is a rectangular matrix whose indices are the left sides of Eqs. (5) and (7), $\mathbf{a}_2 \in \mathbb{R}^{N\times 1}$ is a vector containing $N < M$ impulses that ensure the smoothness of the input shaper, and $\mathbf{b} = \begin{Bmatrix} 0 & 0 & 1 \end{Bmatrix}^T \in \mathbb{R}^{3\times 1}$. The cost function that sums the square difference between the adjacent impulses is defined as:

$$C(\mathbf{a}_2) = \sum_{j=1}^{M-1} \left(A_{j+1} - A_j\right)^2 \tag{9}$$

Therefore, one can find the vector $\mathbf{a}_2$ upon minimizing of the cost function of Eq. (9). The vector containing the three impulses needed to ensure the satisfaction of zero residual vibration of Eq. (7) and the normalization constraint equation of Eq. (5) can then be determined from Eq. (8). It is worth noting that the total shaper duration, $t_M - t_1$, is equal to $(M-1)\Delta t$.

To illustrate this concept, Figure 3 shows different zero-vibration input shaper with a total shaper duration of $\tau_n/2$ and different number of generated impulses in their input shaper's sequence. It is evident that increasing the number of excess impulses does decrease the differences between adjacent impulses. Therefore, when using this generated input shaper to produce a shaped command upon convolution process, the resultant command will have a smooth profile.

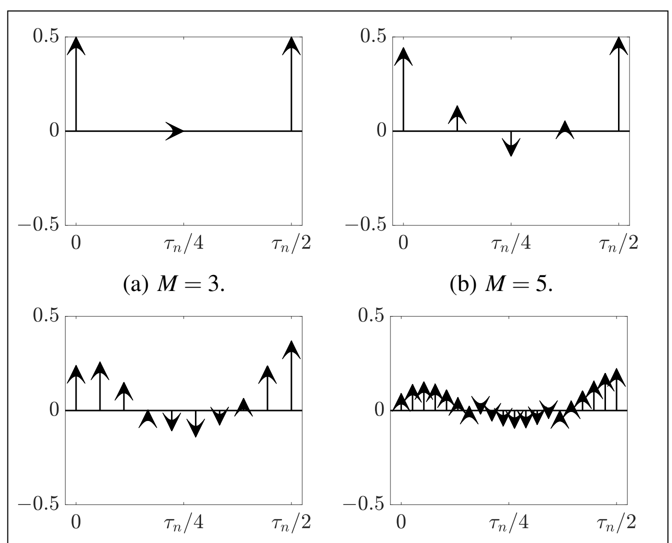

(a) $M = 3$. (b) $M = 5$. (c) $M = 10$. (d) $M = 20$.

Fig. 3: Zero-vibration input shaper with a total shaper duration of $\tau_n/2$ and different number of generated impulses for undamped system ($\zeta_n = 0$); the horizontal arrow corresponds to a zero impulse.

It is clear from Figure 3 that the M-impulse input shaper with $M > 3$ reduces the differences between adjacent impulses and, consequently, decreases the inrush current of the driven actuator compared to the classical two-impulse input shaper shown in Figure 3a. However, this improvement comes at the cost of additional impulses, meaning increased actuation of the driven component of the vibratory system.

IV. SHAPING COMMANDS FROM INPUT SHAPER

To demonstrate the proposed smooth-adjustable multi-impulse input shaper, a unit-step command, $r(t) = H(t)$ where $H(t)$ is the Heaviside function, is used as the reference input. The convolution process is basically summing the products of the impulse A_j with the shifted reference input command by the impulse's time location, i.e., $r(t - t_j)$. Hence,

$$f(t) = s(t) * r(t) = \sum_{j=1}^{M} A_j H(t - t_j) \tag{10}$$

Upon convolving the unit step input, $H(t)$, with the smooth input shaper that is consisted of 20 impulses (see Figure 3d), the convolved command has a smooth profile as depicted in Figure 4. As the number of generated impulses increases in the input shaper, the smoother the shaped command, upon convolution, becomes.

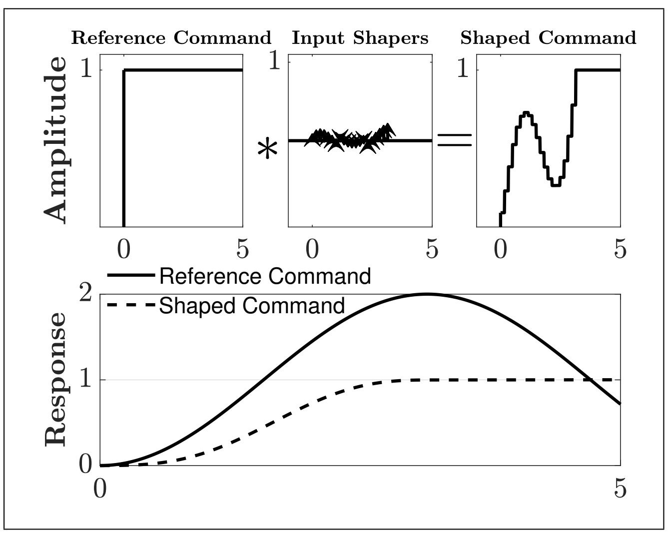

Fig. 4: Convolved smooth shaped command using 20-impulse input shaper from a unit-step reference input command.

V. WATER SLOSHING SUPPRESSION

The proposed controller technique is tested by supressing the induced water sloshing from a laterally-moving container of width W that is filled with a water of depth h.

A. Mathematical Model

The designing of the input shaper requires the system's parameters; natural frequency and damping ratio. The fundamental sloshing frequency of a laterally-moving water-filled container is given as [38]:

$$\omega_n = \sqrt{\frac{\pi g}{W} \tanh\left(\frac{\pi h}{W}\right)} \tag{11}$$

and a damping ratio of $\zeta_n = 0.01$ for water. For small water surface elevations and non-rotational flow, the elevations of the water at one of the corners, $x = 0$ or W in Figure 5, can be given as:

$$\eta(0,t) = \sum_{i=1}^{N} \frac{(2i-1)\pi}{W} \sinh\left(\frac{(2i-1)\pi h}{W}\right) y_i(t) \tag{12}$$

where N is the total modes of the sloshing dynamical model and $y_i(t)$ is the time-dependent amplitude of the sloshing mode i and is determined as the solution of the following second-order differential equation,

$$\ddot{y}_i(t) + 2\zeta_n \omega_n \dot{y}_i(t) + \omega_n^2 y_i(t) = \frac{4W}{(2i-1)^2 \pi^2 \cosh((2i-1)\pi h/W)} \ddot{u}(t) \tag{13}$$

where $\ddot{u}(t)$ is the acceleration of the driven belt that conveys the container.

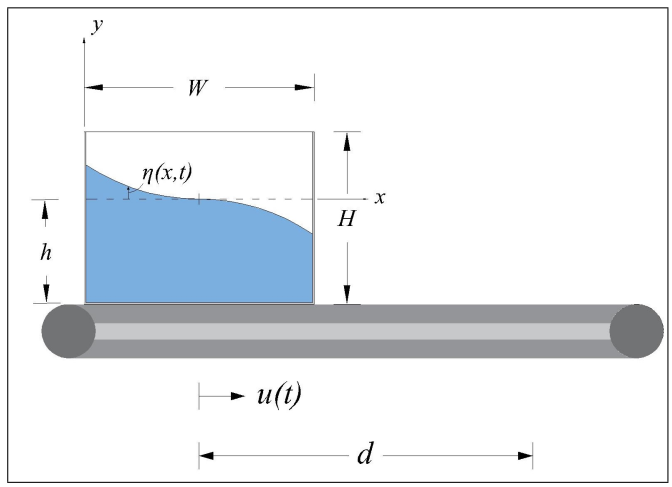

Fig. 5: Laterally-moving container filled with a water of depth h.

B. Numerical Results

The are three phases to move the water-filled container from an initial rest state to a final rest state. The first phase is known as the acceleration phase where the container is commanded to move the container from its rest state to a state with the maximum capability of the driven motor, Figure 6, while suppressing the induced water residual sloshing. Ensuring the driven actuator reaches its maximum capability corresponds to an optimum maneuverability of the moving container. The phase where the container cruises with a constant velocity, and hence no inducing sloshing, prior been commanded to stop is known as the cruising stage. Finally, the phase where the moving container with its maximum driven speed is commanded to decelerate to a complete stop, Figure 6, while suppressing the induced water residual sloshing, is knows as the deceleration phase. The time-optimal rigid-body (TORB) motion with a trapezoidal velocity profile was used as the reference command. It is clear from Figure 6 that the fastest possible way to move a container is by utilizing the motor's maximum acceleration in the acceleration phase to reach the maximum driven velocity in a short time. Similarly, before reaching the target position, distance d in Figure 5, the driven actuator should utilize its maximum deceleration capability to stop the container in a short time.

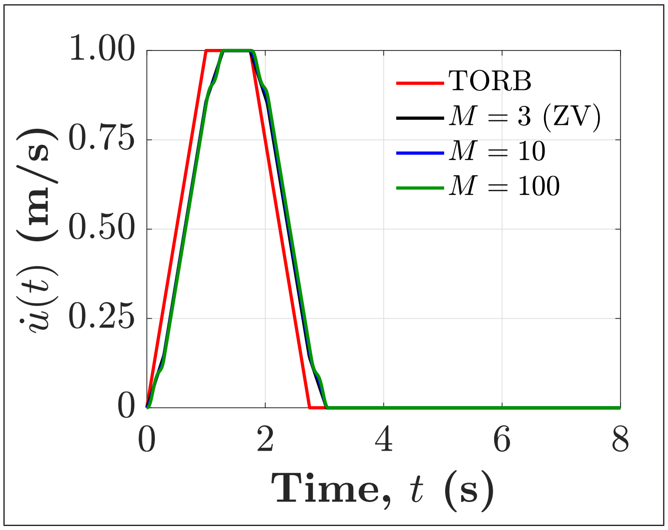

Fig. 6: Input shaped velocity command, $\dot{u}(t)$, of the moving container designed using zero-residual vibration constraints, different number of impulses M, and a shaper duration of $t_M = \tau_d/2$.

The corresponding numerically-predicted free-surface elevation, $\eta(0,t)$, of the moving water-filled container when it is subjected by the velocity command of Figure 6 is shown in Figure 7. It is clear that the shaped command suppresses the induced sloshing even though only the fundamental sloshing mode was used in the designing the input shaper. Even though one can enhance the shaper robustness or considering the higher sloshing modes in the designing process, the objective of the current simulation experiment is to show the efficacy of the proposed smooth input-shaping technique to limit the residual vibration (sloshing in the current example) compared to the classical ZV input shaper.

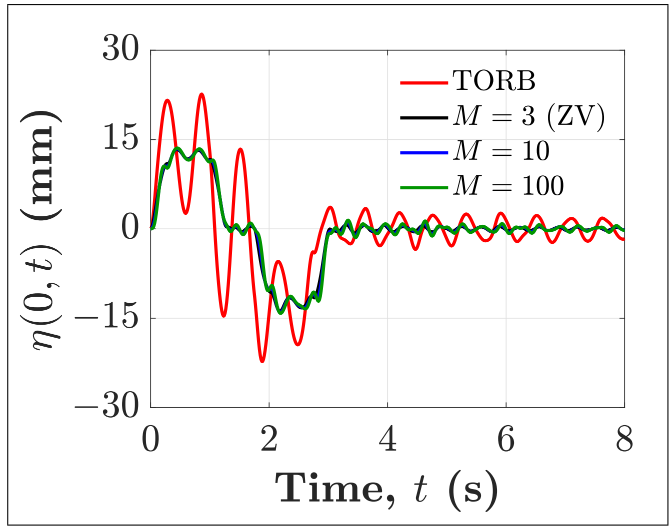

Fig. 7: The corresponding numerically-predicted free-surface elevation, $\eta(0,t)$, of the moving water-filled container when it is subjected by the velocity command of Figure 6.

VI. CONCLUSIONS

The input shaping control was improved to shape a smooth command regardless the reference input used to command a flexible vibratory system. The proposed control technique introduces a multi-impulse input shaper that, upon convolution, generates a smooth shaped command without compromising the total maneuver time by fully utilizing the system's maximum input capability. The performance of the adjustable-smooth multi-impulse input shaper is tested by numerically suppressing the induced sloshing of a laterally-moving water-filled container, while only considering the fundamental mode of the multi-mode sloshing dynamical system.

The proposed input-shaping technique can be extended to a multi-mode system by enforcing the conditions of Eq. (7) to each vibrational mode of the considered flexible multi-mode system. Furthermore, the robustness to system uncertainties can be enhanced by imposing additional constraints beyond Eq. (7).

ACKNOWLEDGMENT

We wish to acknowledge the support of Kuwait Foundation for the Advancement of Sciences (KFAS).

REFERENCES

[1] W. Yang, S. Li, and X. Luo, "Data Driven Vibration Control: A Review," in IEEE/CAA Journal of Automatica Sinica, vol. 11, no. 9, pp. 1898-1917, 2024.

[2] J. Lawrence and W. Singhose, "Command Shaping Slewing Motions for Tower Cranes," Journal of Vibration and Acoustics, vol. 132, no. 1, Jan. 2010.

[3] H. Chen, Y. Fang, and N. Sun, "An adaptive tracking control method with swing suppression for 4-DOF tower crane systems," Mechanical Systems and Signal Processing, vol. 123, pp. 426–442, May 2019.

[4] H. D. Tho, K. Terashima and T. Miyoshi, "Oscillation Control of a Double-Pendulum Overhead Crane based on Model-Matching Input Shaping Technique," 2024 IEEE International Conference on Advanced Intelligent Mechatronics (AIM), Boston, MA, USA, 2024, pp. 765-770.

[5] J.-K. Cho and Y.-S. Park, "Vibration reduction in flexible systems using a time-varying impulse sequence," Robotica, vol. 13, no. 3, pp. 305–313, 1995.

[6] Z. Mohamed, J. M. Martins, M. O. Tokhi, J. Sá da Costa, and M. A. Botto, "Vibration control of a very flexible manipulator system," Control Engineering Practice, vol. 13, no. 3, pp. 267–277, Mar. 2005.

[7] AA. Alshaya and K. Alghanim, "Command Shaping for Sloshing Suppression of a Suspended Liquid Container," Journal of Dynamic Systems, Measurement, and Control, vol. 142, no. 121003, 2020.

[8] N. C. Singer and W. P. Seering, "Experimental Verification of Command Shaping Methods for Controlling Residual Vibration in Flexible Robots," 1990 American Control Conference, pp. 1738–1744, 1990.

[9] N. C. Singer, and W. P Seering, "Preshaping Command Inputs to Reduce System Vibration, in Journal of Dynamic Systems, Measurement, and Control," vol. 112, no. 1, pp. 76–82, 1990.

[10] R. Zhang, "Research on Vibration Suppression Algorithm Based on Continuous Input Shaping," 2024 3rd International Conference on Robotics, Artificial Intelligence and Intelligent Control (RAIIC), Mianyang, China, 2024, pp. 308-312.
[11] H. P. Nguyen, N. T. Bui and T. v. A. Nguyen, "Tracking Control Based on Takagi-Sugeno Fuzzy Descriptor Model for Overhead Crane Combined With Input Shaping," in IEEE Access, vol. 12, pp. 127507-127521, 2024.
[12] H. Bilal, M. S. Aslam, Y. Tian, A. Yahya and B. Abu Izneid, "Enhancing Trajectory Tracking and Vibration Control of Flexible Robots With Hybrid Fuzzy ADRC and Input Shaping," in IEEE Access, vol. 12, pp. 150574-150591, 2024.
[13] W. Singhose and L. Pao, "A comparison of input shaping and time-optimal flexible-body control," Control Engineering Practice, vol. 5, no. 4, pp. 459–467, Apr. 1997.
[14] N. C. Singer and W. P. Seering, "An extension of command shaping methods for controlling residual vibration using frequency sampling," in Proceedings 1992 IEEE International Conference on Robotics and Automation, May 1992, pp. 800–805 vol.1.
[15] J. Vaughan, A. Yano, and W. Singhose, "Comparison of robust input shapers," Journal of Sound and Vibration, vol. 315, no. 4, pp. 797–815, Sep. 2008.
[16] D. Blackburn et al., "Command Shaping for Nonlinear Crane Dynamics," Journal of Vibration and Control, vol. 16, no. 4, pp. 477–501, Apr. 2010.
[17] Z. Mohamed and M. Tokhi, "Command shaping techniques for vibration control of a flexible robot manipulator," Mechatronics, vol. 39, pp. 1039–1047, Jan. 2003.
[18] S. M. Fasih ur Rehman, Z. Mohamed, A. R. Husain, H. I. Jaafar, M. H. Shaheed, and M. A. Abbasi, "Input shaping with an adaptive scheme for swing control of an underactuated tower crane under payload hoisting and mass variations," in Mechanical Systems and Signal Processing vol. 175 pp. 109106, 2022.
[19] J. M. Hyde and W. P. Seering, "Using input command pre-shaping to suppress multiple mode vibration," in Proceedings. 1991 IEEE International Conference on Robotics and Automation, Sacramento, CA, USA, USA: IEEE, 1991, pp. 2604–2609 vol.3.
[20] R. Kumar and T. Singh, "Design of input shapers using modal cost for multi-mode systems," in Proceedings of the 2010 American Control Conference, Jul. 2010, pp. 2290–2295.
[21] M.-C. Pai, "Robust input shaping control for multi-mode flexible structures," International Journal of Control, Automation and Systems, vol. 9, no. 1, pp. 23–31, Feb. 2011.
[22] H. Yavuz, S. Mıstıkoğlu, and S. Kapucu, "Hybrid input shaping to suppress residual vibration of flexible systems," Journal of Vibration and Control, vol. 18, no. 1, pp. 132–140, Jan. 2012.
[23] W. Singhose, L. Porter, M. Kenison, and E. Kriikku, "Effects of hoisting on the input shaping control of gantry cranes," Control Engineering Practice, vol. 8, no. 10, pp. 1159–1165, Oct. 2000.
[24] D. K. Thomsen, R. Se-Knudsen, D. Brandt, O. Balling, and X. Zhang, "Smooth online time-varying input shaping with fractional delay FIR filtering," Control Engineering Practice, vol. 88, pp. 21–37, Jul. 2019.
[25] [19] D. K. Thomsen, R. Se-Knudsen, O. Balling, and X. Zhang, "Vibration control of industrial robot arms by multi-mode time-varying input shaping," Mechanism and Machine Theory, vol. 155, p. 104072, Jan. 2021.
[26] S. Arabasi and Z. Masoud, "Frequency-Modulation Input-Shaping Strategy for Double-Pendulum Overhead Cranes Undergoing Simultaneous Hoist and Travel Maneuvers," IEEE Access, vol. 10, pp. 44954–44963, 2022.
[27] W. Singhose, R. Eloundou, and J. Lawrence, "Command Generation for Flexible Systems by Input Shaping and Command Smoothing," Journal of Guidance, Control, and Dynamics, vol. 33, no. 6, pp. 1697–1707, Nov. 2010.
[28] B. Pridgen and W. Singhose, "Comparison of Polynomial Cam Profiles and Input Shaping for Driving Flexible Systems," Journal of Mechanical Design, vol. 134, no. 12, Nov. 2012.
[29] X. Xie, J. Huang, and Z. Liang, "Vibration reduction for flexible systems by command smoothing," Mechanical Systems and Signal Processing, vol. 39, no. 1, pp. 461–470, Aug. 2013.
[30] A. Alshaya and A. Alshayji, "Robust multi-steps input command for liquid sloshing control," Journal of Vibration and Control, p. 10775463211017721, 2021.
[31] A. Alshaya and D. Almujarrab, "A smooth polynomial shaped command for sloshing suppression of a suspended liquid container," Transactions of the Institute of Measurement and Control, vol. 43, no. 2, pp. 278–294, 2020.
[32] A. Alshaya and K. Alhazza, "Smooth and robust multi-mode shaped commands," Mechanical Systems and Signal Processing, vol. 168, p. 108658, 2022.
[33] K. A. Alhazza and Z. N. Masoud, "Waveform command shaping control of multimode systems," Journal of Sound and Vibration, vol. 363, pp. 126–140, 2016.
[34] K. Alhazza, Z. Masoud, and N. Alotaibi, "A Smooth Wave-Form Shaped Command with Flexible Maneuvering Time: Analysis and Experiments," Asian Journal of Control, vol. 18, no. 4, pp. 1376–1384, 2016.
[35] K. A. Alhazza, "Adjustable maneuvering time wave-form command shaping control with variable hoisting speeds," Journal of Vibration and Control, vol. 23, no. 7, pp. 1095–1105, 2017.
[36] A. Alshaya, "Command Shaping Control of a Multi-Mode Flexible System," in 2022 8th International Conference on Control, Decision and Information Technologies (CoDIT), May 2022, pp. 206–211.
[37] A. A. Alshaya, "Vibration Control of Time-Varying Nonlinear Systems," in Advances in Nonlinear Dynamics, Volume II, W. Lacarbonara, Ed., Cham: Springer Nature Switzerland, 2024, pp. 15–24.
[38] R. A. Ibrahim, Liquid Sloshing Dynamics: Theory and Applications, 1 edition. New York: Cambridge University Press, 2005.